First-Order Phase Transition in a Model Glass Former: Coupling of Local Structure and Dynamics

Thomas Speck,[1] Alex Malins,[2,3] and C. Patrick Royall[2,4,5]

[1]*Institut für Theoretische Physik II, Heinrich-Heine-Universität, D-40225 Düsseldorf, Germany*
[2]*School of Chemistry, University of Bristol, Bristol BS8 1TS, United Kingdom*
[3]*Bristol Centre for Complexity Sciences, University of Bristol, Bristol BS8 1TS, United Kingdom*
[4]*HH Wills Physics Laboratory, University of Bristol, Bristol BS8 1TL, United Kingdom*
[5]*Centre for Nanoscience and Quantum Information, Bristol BS8 1FD, United Kingdom*

(Received 26 July 2012; published 8 November 2012)

Recently, numerical evidence for a dynamical first-order phase transition in trajectory space [L. O. Hedges *et al.*, Science **323**, 1309 (2009)] has been found. In a model glass former in which clusters of 11 particles form upon cooling, we find that the transition has both dynamical and structural character. It occurs between an active phase with a high fraction of mobile and low fraction of cluster particles, and an inactive phase with few mobile but many cluster particles. The transition can be driven *both* dynamically and structurally with a chemical potential, showing that local order forms a mechanism for dynamical arrest.

DOI: 10.1103/PhysRevLett.109.195703 PACS numbers: 64.70.Q−

Introduction.—Understanding the glass transition is a long-standing challenge of condensed matter physics [1]. In particular, describing the transition from liquid to solid (from a dynamical perspective) without significant change in structure has eluded a convincing theoretical description. Until recently, it was believed that there was very little change in structure upon quenching a liquid into a glass. This was based upon evidence from both experiment and simulation [1]. However, such evidence focused on pair correlations.

As far back as 1952, Frank argued that higher-order structural motifs might become prevalent in glass-forming liquids upon quenching [2]. These predictions have now been realized, with higher-order motifs found in a variety of glass-forming liquids [3–11]. While it has thus emerged that deeply supercooled liquids and glasses certainly exhibit ordering and are far from being structurally indistinguishable from liquids, only in a few cases has a causal link between structure and arrest been made [4,5,8,9]. Moreover, the opposite has also been claimed [12]. It would thus be most attractive to settle the conundrum about structure and the glass transition. In this Letter, we take a step in this direction and use a structural mechanism to drive a first-order phase transition in trajectory space. In particular, we change the chemical potential of the structural motif associated with slow dynamics in a model glass former.

Dynamical phase transitions have been found analytically and numerically in kinetically constrained lattice models [13–15]. Hedges *et al.* showed that a similar first-order transition exists in an atomistic model glass former [16]. In all of these models, the distributions of suitable order parameters manifesting dynamic heterogeneities show that low mobility, or activity, is more probable than what would be expected from a Gaussian distribution. These low activity tails can be enhanced through a biasing field s, which couples linearly to the order parameter much in analogy to conventional thermodynamics, where, e.g., an external field couples to the magnetization. The transition then occurs between the normal liquid, or *active phase*, and an *inactive phase* comprised of trajectories in which particles maintain a high overlap with their initial positions.

It has been shown very recently that the inactive states formed in this s ensemble have lower potential energies, and exhibit very slow dynamics even when run without biasing ($s = 0$) before ''melting'' back into the liquid state [17,18]. Given the interest in structure and the glass transition, it seems tempting to look for structural motifs in the inactive states formed in the s ensemble. While we begin with such an analysis, we go further: in addition to biasing with the dynamical quantity s, we bias with μ, the dynamical chemical potential of the bicapped square antiprism clusters that we refer to as 11*A* [19]. The population of these clusters is known to increase on cooling in the Kob-Andersen glass former that we simulate [3]; see Fig. 1(b). Remarkably, we find that both s and our structural parameter μ drive the same dynamical phase transition.

Model.—We study the popular Kob-Andersen (KA) binary mixture, which is composed of large (A) particles and small (B) particles interacting through Lennard-Jones potentials [21] (see the Supplemental Material [22]). Throughout the Letter, we employ reduced Lennard-Jones units with respect to the large particles. An analysis of the system is presented in Fig. 1 for a total number of $N = 10976$ particles at number density $N/V = 1.2$. We determine the structural relaxation time τ_α from the decay of the intermediate scattering function

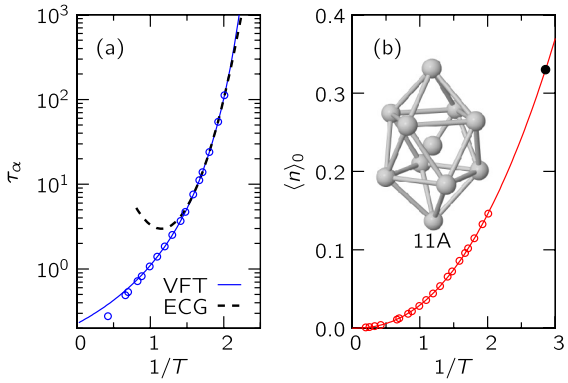

FIG. 1 (color online). (a) Structural relaxation time τ_α vs inverse temperature $1/T$. Open circles are numerical data. The solid line is the Vogel-Fulcher-Tammann (VFT) fit, the dashed line is the Elmatad-Chandler-Garrahan (ECG) fit holding for $T < T_0$. (b) Mean population $\langle n\rangle_0$ of $11A$ clusters (see the inset picture). The filled circle shows the largest population ($\simeq 0.33$) of $11A$ clusters we have reached in the simulations. Using a power law extrapolation (line) implies a fictive temperature $T \simeq 0.35$.

$F_A(t) = \sum_k \langle e^{i\mathbf{q}\cdot[\mathbf{r}_k(t)-\mathbf{r}_k(0)]}\rangle_0/N_A$ through $F_A(\tau_\alpha) = 1/e$ at wave vector $|\mathbf{q}| \simeq 7.21$ corresponding to the first peak of the structure factor. The brackets $\langle \ldots \rangle$ denote an average, whereas the subscript 0 emphasizes that no biasing field is applied. The structural relaxation time is plotted in Fig. 1(a) as a function of temperature together with two functional forms that fit our relaxation data similarly well: (i) The Vogel-Fulcher-Tammann expression $\tau_\alpha \propto \exp\{A/(T - T_{\mathrm{VFT}})\}$ yielding $T_{\mathrm{VFT}} \simeq 0.325$ [23,24], and (ii) the parabolic Elmatad-Chandler-Garrahan fit $\tau_\alpha \propto \exp\{(J/T_0)^2(T_0/T - 1)^2\}$ holding below the onset temperature $T_0 \simeq 0.87$ [25] (A and J are additional fit parameters). While T_0 marks the onset of dynamical heterogeneity and is a material property, $T_{\mathrm{VFT}} \ll T_0$ is often associated with an ideal glass transition temperature [1], but depends on the range of data fitted [26].

In Fig. 1(b), the population of particles in $11A$ clusters, $\langle n\rangle_0$, is shown as a function of temperature. Clusters are detected from the real positions $\{\mathbf{r}_k\}$ using the topological cluster classification (TCC), where a Voronoi construction is used to detect the neighbor network [9]. Note that the actual clusters can overlap so that one particle can be a member of more than one cluster. No distinction between A and B particles is made in the cluster detection. There is a clear increase in the population of $11A$ as the system is cooled. We fit the $11A$ population with an empirical power law $\langle n\rangle_0 = 0.029T^{-2.3}$ [solid line in Fig. 1(b)]. Of course, such a dependence cannot describe the whole range since the population cannot exceed unity. Thus, $11A$ can be argued to be coupled to the increasingly slow dynamics in the supercooled KA liquid. This finding is consistent with that of Coslovich and Pastore [3]. By comparison, the populations of other clusters (including a cluster similar in size to $11A$) show a much weaker temperature dependency and are not associated with the slow dynamics (see the Supplemental Material [22]).

Biased simulations.—In the following, we employ the techniques described in more detail in Ref. [18] and, therefore, here we only give a brief overview. In particular, throughout the remainder of this Letter, we study a small system with $N = 216$ particles at a modestly supercooled state point with density $N/V = 1.2$ and temperature $T = 0.6$. We use NVT molecular dynamics simulations to harvest trajectories of length $t_{\mathrm{obs}} = K\Delta t$, where $K + 1$ configurations are stored at regular times $t_i = i\Delta t$.

We analyze trajectories on the fly and calculate two order parameters along each trajectory. First, we obtain the total number $\mathcal{C} = \sum_{ik} h_k^m(t_i)$ of mobile particles. Here, $h_k^m(t) = \Theta(|\hat{\mathbf{r}}_k(t) - \hat{\mathbf{r}}_k(t - \Delta t)| - a)$ is 1 if particle k has moved further than $a = 0.3$ with respect to its inherent state position $\hat{\mathbf{r}}_k$ (as obtained from a steepest descent quench), and 0 otherwise. We employ inherent state positions to filter vibrations and focus on long-lived particle displacement, whereby the commitment time $\Delta t = 1.5$ is chosen in order to allow particles to commit to a new position [27]. Second, from the real positions $\{\mathbf{r}_k\}$ we determine the total number of particles $\mathcal{N} = \sum_{ik} h_k^{11A}(t_i)$ bound in $11A$ clusters, where h_k^{11A} is 1 if particle k is part of a cluster and 0 otherwise.

Our central quantities of interest are the fraction of mobile particles $c = \mathcal{C}/(NK)$ and the fraction of particles identified within $11A$ clusters $n = \mathcal{N}/[N(K + 1)]$. Sampling of the tails of the distributions $p(c)$ and $p(n)$ requires us to employ importance sampling combining replica exchange with moves borrowed from transition path sampling [28]. This allows us to reweight trajectories and to analyze our data in terms of dynamical ensembles in which an external field couples to an order parameter. In particular, for an observable $\mathcal{O}$ we define two ensembles

$$\langle \mathcal{O}\rangle_s = \frac{\langle \mathcal{O}e^{-s\mathcal{C}}\rangle_0}{\langle e^{-s\mathcal{C}}\rangle_0}, \qquad \langle \mathcal{O}\rangle_\mu = \frac{\langle \mathcal{O}e^{\mu\mathcal{N}}\rangle_0}{\langle e^{\mu\mathcal{N}}\rangle_0}, \tag{1}$$

with biasing fields s and μ, respectively. Hence, positive biasing fields enhance the weight of trajectories that have fewer mobile or more cluster particles, respectively. Treating cluster particles as a species, and for Δt large such that configurations sampled at times t_i are independent, the field μ becomes the chemical potential for the $11A$ particles. Of course, here it denotes the dynamical analog since configurations are correlated along trajectories.

For each set of parameters, we have harvested 3×10000 trajectories after the system has relaxed. Errors are estimated as the standard deviation calculated from splitting the data into three sets of 10000 trajectories. In order to calculate distributions and averages we employ the multistate Bennett acceptance ratio method [29,30]. We do not restrict the trajectories we accept in our importance

sampling scheme, in particular, we might accept trajectories that have crystallized. However, we did not observe such an event and all structural measures show that the prepared inactive phase is amorphous (see the Supplemental Material [22]). Moreover, 11*A* clusters are not part of the KA ground state [31] and we expect that their formation rather competes with than promotes crystallization [3].

Results.—Given the structural response of the KA mixture to cooling, it is natural to enquire as to its relation with the first-order dynamical transition in trajectory space. In Figs. 2(a)–2(c), we show the result for the s ensemble [18] obtained from two runs with trajectory lengths $K = 100$ and $K = 200$, respectively. In Fig. 2(a), the probability distribution of c is shown, which becomes nonconcave (it acquires a shoulder) for trajectories of length $K = 200$. The external field s coupling to the order parameter tilts this distribution until at $s^* \simeq 0.0034$ the fluctuations $\langle c^2\rangle_s - \langle c\rangle_s^2$ are maximized and $\ln p(c) - s^* c$ exhibits a bimodal shape, see Fig. 2(b), indicating a first-order dynamical phase transition. The effect of varying the biasing field s on mobility is shown in Fig. 2(c), exhibiting a transition from an active phase to an inactive phase. Simultaneously, we show the effect on the structure. We see that 11*A* cluster populations are inversely correlated with the active and inactive phases. In other words, the glassy inactive states have a higher 11*A* population. Moreover, comparison with other clusters show less change across the transition (see the Supplemental Material [22]).

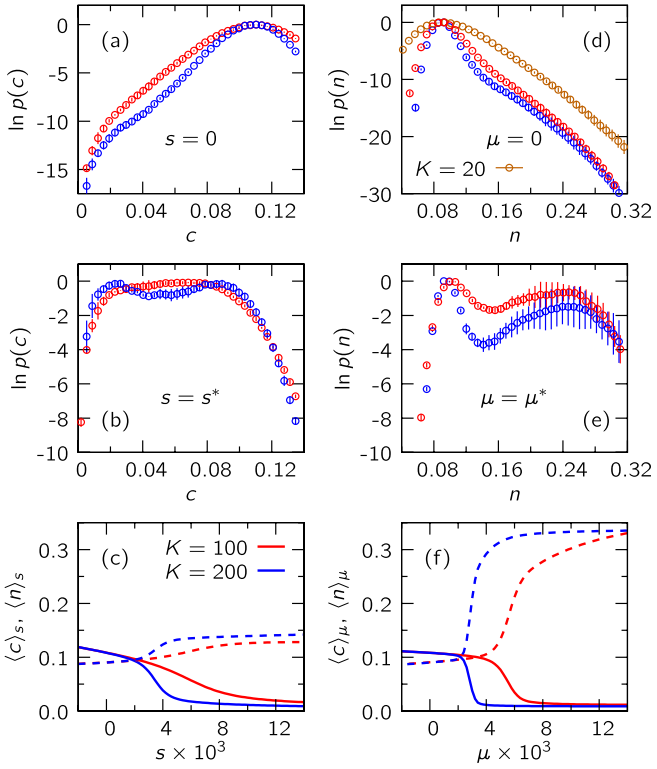

FIG. 2 (color online). Left column: s ensemble (a) Probability distributions $p(c)$ for the density of mobile particles c for two trajectory lengths. The nonconcave shape indicates a phase transition in trajectory space as becomes obvious from the bimodal distribution (b) at the field s^* that maximizes the fluctuations $\langle c^2\rangle_s - \langle c\rangle_s^2$. (c) Average fractions of mobile particles (solid lines) and 11*A* cluster population (dashed lines) vs the biasing field s. Right column: (d)–(f) as left column but for the μ ensemble. Throughout, bright (red) and dark (blue) lines refer to $K = 100$ and $K = 200$, respectively, with an additional data set $K = 20$ in (d).

Having demonstrated that the inactive and active phases are structurally distinct, we enquire whether structure itself in the form of 11*A* clusters can be used as an order parameter to drive such a dynamical transition. As shown in Figs. 2(d)–2(f) this is indeed the case. The distribution $p(n)$ [Fig. 2(d)] acquires a nonconcave shape already for $K = 100$. In Fig. 2(e), we plot the reweighted distributions at μ^* maximizing the fluctuations $\langle n^2\rangle_\mu - \langle n\rangle_\mu^2$. The effect of varying μ shown in Fig. 2(f) is similar to s; i.e., there is a sudden drop of the fraction of mobile particles c accompanied by an increase of n. However, the effect on the 11*A* cluster population is rather stronger, leading to a cluster-rich phase with $\langle n\rangle_\mu$ exceeding >0.3 in contrast to $\langle n\rangle_s \simeq 0.14$ for the inactive phase. We have thus shown that both stuctural and dynamical biasing fields lead to similar dynamical phase transitions. As we shall see below, both properties are actually manifestations of the same transition.

To study the global structure and dynamics, we have harvested trajectories with $K = 100$ in the unbiased ensemble ($\mu = 0$) and at constant external field $\mu = 0.014 > \mu^* \simeq 0.0056$ deep in the cluster-rich phase. The population of 11*A* clusters is $\langle n\rangle_{0.014} \simeq 0.33$, a value that, following the power law fit, corresponds to a "fictive" temperature $T \simeq 0.35$ [see Fig. 1(b)] close to the VFT temperature. Similar to the s ensemble [16,18], the pair distribution function for the large (A) particles is virtually indistinguishable between unbiased and biased ensemble. However, changes are observed for the small (B) particles in Fig. 3(b), indicating an excess of B-B bonds sharing 3 common A neighbors [32]. To show that the cluster-rich phase not only has a small number of mobile particles but also relaxes much slower, we show in Fig. 3(c) the intermediate scattering function $F_A(t)$, where the sum runs over all A particles. It is evident that particles in the cluster-rich phase maintain a high overlap with their initial positions, preventing the system from relaxing.

To complete our analysis, we study the melting of the μ ensemble. To this end, we take cluster-rich configurations from the center of trajectories sampled at $\mu = 0.014$ and run them evolving under the unbiased dynamics. We average over 500 runs for each of these configurations. The curve shown in Fig. 3(d) is the result after averaging over 31 uncorrelated cluster-rich configurations. With a relaxation time of $\tau_\alpha \simeq 545$, these configurations relax markedly

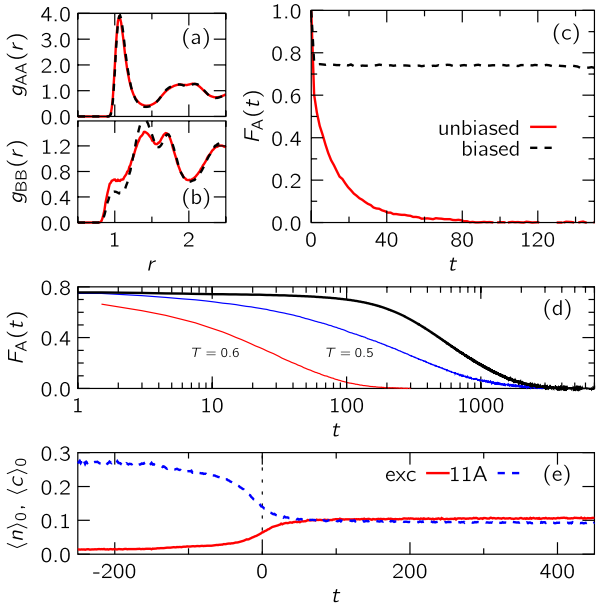

FIG. 3 (color online). Radial distribution functions for (a) the large A particles and (b) the small B particles for both the unbiased ensemble ($\mu = 0$, solid line) and in the inactive phase ($\mu = 0.014 > \mu^*$, dashed line). (c) The intermediate scattering function (ISF) for the A particles. (d) Slow decay of the ISF for the melting runs (black line). Also shown are the ISFs for equilibrated systems at $T = 0.6$ and the lower temperature $T = 0.5$. (e) Time evolution of mobile (solid line) and cluster particle (dashed line) populations, where $t = 0$ corresponds to the interface.

slower than an equilibrium system at the lower temperature $T = 0.5$, but are comparable to initial configurations taken from the s ensemble [17]. Single runs show an "interface" in space-time; i.e., the intermediate scattering function drops abruptly from $\simeq 0.8$ to zero at some waiting time. For all runs, we determine this waiting time from fitting $F_A(t)$ with a tanh function. Figure 3(e) finally shows the temporal evolution of mean mobile and cluster particle populations, where single runs are shifted such that $t = 0$ corresponds to the waiting time. Clearly, at the time the intermediate scattering function decays the number of mobile particles suddenly rises while the $11A$ population drops.

We have demonstrated that the dynamical properties of the cluster-rich phase are very similar to the inactive phase. Indeed, combining the numerical data from both order parameters to obtain the two-dimensional joint probability $p(n, c)$ shown in Fig. 4 we discern only two basins implying that inactive and cluster-rich phase coincide. Consequently, the dynamical transition is the same whether it is driven through s or μ, which is the central result of this Letter. The active phase is found at large c and small n; the inactive phase is found at small c and large n. The actual reaction coordinate determining the height of the barrier at coexistence the system has to cross is a combination of, at least, c and n. Note that both $p(c)$

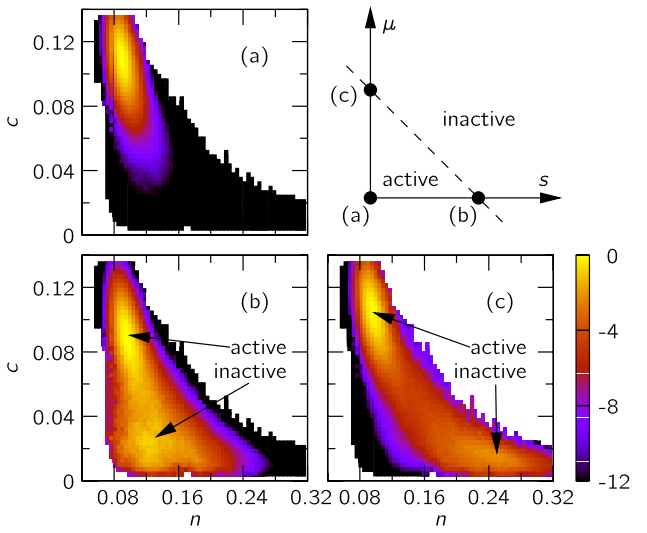

FIG. 4 (color online). Logarithm of the joint probability $p(n, c)$ shown for (a) the unbiased ensemble and at coexistence in (b) the dynamical s ensemble ($s = s^*$) and (c) the structural μ ensemble ($\mu = \mu^*$) for trajectory length $K = 200$ (all plots show the same data reweighted differently). The phase diagram in the s-μ plane is sketched in the upper corner.

and $p(n)$ are projections (i.e., marginal distributions) of this joint distribution.

Even though there is only a single basin for the inactive phase in Fig. 4(b), it is considerably broader (along the n axis) than the active phase allowing for larger fluctuations. This might indicate that the formation of $11A$ clusters, while able to control dynamics, is not the only mechanism of slow glassy dynamics. Whereas, the probability sharply drops as c approaches zero, the cluster population can vary greatly in the two ensembles since going to larger n the decay of the probability $p(n)$ is more gradual with a long tail. Hence, even after reaching the inactive phase, we can force the system to organize more and more particles into $11A$ clusters, but it cannot become any "slower" (in the sense that the intermediate scattering function does not decay in the inactive phase on the simulation time scale).

Conclusions.—In summary, we have performed a structural analysis of active and inactive trajectories sampled by biasing with the density of mobile particles [18]. Our analysis has revealed that the glassy states have a higher population of bicapped square antiprism ($11A$) clusters compared to the liquid. Coupling the trajectories to a structural biasing field μ based on the $11A$ population results in the same first-order transition in structure and mobility as when biasing with the mobility field s [16,18]. In other words, the first-order phase transition in trajectory space has both structural and dynamic characteristics. That this transition can also be driven by the chemical potential of $11A$ cluster particles gives strong evidence that, at least in this system, which is accepted to be representative of a wide range of glass formers, structure forms a mechanism for dynamical arrest.

Is the inactive phase related to state points at lower temperatures? The fact that the same cluster type 11*A* shows an increase of its population both when cooling the system and when biasing with dynamics seems to supports this idea. Although the system cannot become measurable slower on the simulation time scale, it is tempting to suppose that, if $\langle n \rangle_0$ is an order parameter for how glassy the system is, a much higher $\langle n \rangle_\mu$ in the μ ensemble corresponds to a remarkably supercooled state. The fact that the transition is absent for short trajectories [cf. Fig. 2(d)] indicates that dynamical correlations are at play. However, we cannot exclude the possibility that this is a finite size effect and that very large systems display a conventional order-disorder transition with the population of 11*A* clusters serving as an order parameter. Biasing with a predefined local motif can be understood as constraining the relative positions of particles. Although this is a much weaker condition compared to pinning a subset of particles, a connection with the random pinning glass transition [33] is conceivable.

Since 11*A* clusters allow the system to reduce its potential energy, one would indeed expect that their formation is promoted at low temperatures. However, we have shown that even at modestly supercooled conditions and constant temperature, these clusters are rather easily induced and are able to dramatically influence the dynamic properties of the liquid. The controlling of amorphous short-range order thus opens a route towards "high temperature glasses" that are prepared by means other then a temperature quench.

We thank David Chandler, Bob Evans, Rob Jack, Jens Eggers, Hartmut Löwen, and Stephen Williams for enlightening discussions. Financial support by the Humboldt foundation (T. S.), EPSRC (A. M.—Grant No. EP/E501214/1), and the Royal Society (C. P. R.) is gratefully acknowledged. This work was carried out using the computational facilities of the Advanced Computing Research Centre, University of Bristol.

[1] L. Berthier and G. Biroli, Rev. Mod. Phys. **83**, 587 (2011).
[2] F. C. Frank, Proc. R. Soc. A **215**, 43 (1952).
[3] D. Coslovich and G. Pastore, J. Chem. Phys. **127**, 124504 (2007).
[4] M. Dzugutov, S. I. Simdyankin, and F. H. M. Zetterling, Phys. Rev. Lett. **89**, 195701 (2002).
[5] A. Malins, J. Eggers, C. P. Royall, S. R. Williams, and H. Tanaka, arXiv:1203.1732.
[6] H. Jonsson and H. C. Andersen, Phys. Rev. Lett. **60**, 2295 (1988).
[7] F. Sausset, G. Tarjus, and P. Viot, Phys. Rev. Lett. **101**, 155701 (2008).
[8] H. Tanaka, T. Kawasaki, H. Shintani, and K. Watanabe, Nature Mater. **9**, 324 (2010).
[9] C. P. Royall, S. R. Williams, T. Ohtsuka, and H. Tanaka, Nature Mater. **7**, 556 (2008).
[10] U. R. Pedersen, T. B. Schroder, J. C. Dyre, and P. Harrowell, Phys. Rev. Lett. **104**, 105701 (2010).
[11] A. J. Dunleavy, K. Wiesner, and C. P. Royall, arXiv:1205.0187.
[12] B. Charbonneau, P. Charbonneau, and G. Tarjus, Phys. Rev. Lett. **108**, 035701 (2012).
[13] M. Merolle, J. P. Garrahan, and D. Chandler, Proc. Natl. Acad. Sci. U.S.A. **102**, 10 837 (2005).
[14] J. P. Garrahan, R. L. Jack, V. Lecomte, E. Pitard, K. van Duijvendijk, and F. van Wijland, Phys. Rev. Lett. **98**, 195702 (2007).
[15] J. P. Garrahan, R. L. Jack, V. Lecomte, E. Pitard, K. van Duijvendijk, and F. van Wijland, J. Phys. A **42**, 075007 (2009).
[16] L. O. Hedges, R. L. Jack, J. P. Garrahan, and D. Chandler, Science **323**, 1309 (2009).
[17] R. L. Jack, L. O. Hedges, J. P. Garrahan, and D. Chandler, Phys. Rev. Lett. **107**, 275702 (2011).
[18] T. Speck and D. Chandler, J. Chem. Phys. **136**, 184509 (2012).
[19] The 11*A* cluster is equivalent to the (0,2,8) Voronoi polygon seen in Ref. [3]. We follow the naming convention of Ref. [20].
[20] J. P. K. Doye, D. J. Wales, and R. S. Berry, J. Chem. Phys. **103**, 4234 (1995).
[21] W. Kob and H. C. Andersen, Phys. Rev. Lett. **73**, 1376 (1994).
[22] See Supplemental Material at http://link.aps.org/supplemental/10.1103/PhysRevLett.109.195703 for methods and additional data.
[23] A. Cavagna, Phys. Rep. **476**, 51 (2009).
[24] S. Sastry, Nature (London) **409**, 164 (2001).
[25] Y. S. Elmatad, D. Chandler, and J. P. Garrahan, J. Phys. Chem. B **113**, 5563 (2009).
[26] Y. S. Elmatad, D. Chandler, and J. P. Garrahan, J. Phys. Chem. B **114**, 17113 (2010).
[27] A. S. Keys, L. O. Hedges, J. P. Garrahan, S. C. Glotzer, and D. Chandler, Phys. Rev. X **1**, 021013 (2011).
[28] P. G. Bolhuis, D. Chandler, C. Dellago, and P. L. Geissler, Annu. Rev. Phys. Chem. **53**, 291 (2002).
[29] M. R. Shirts and J. D. Chodera, J. Chem. Phys. **129**, 124105 (2008).
[30] D. D. L. Minh and J. D. Chodera, J. Chem. Phys. **131**, 134110 (2009).
[31] J. R. Fernández and P. Harrowell, Phys. Rev. E **67**, 011403 (2003).
[32] J. R. Fernández and P. Harrowell, J. Phys. Chem. B **108**, 6850 (2004).
[33] C. Cammarota and G. Biroli, Proc. Natl. Acad. Sci. U.S.A. **109**, 8850 (2012).